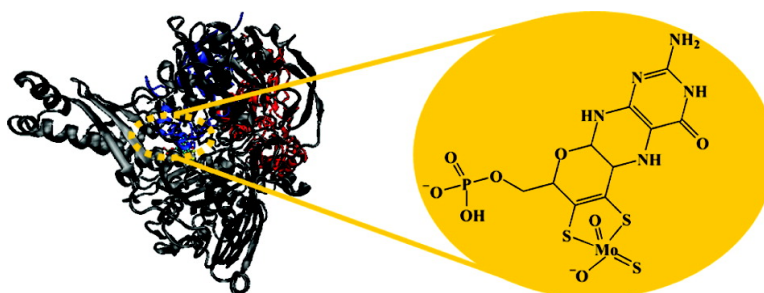


## Oxidation Reaction by Xanthine Oxidase. Theoretical Study of Reaction Mechanism

Tatsuo Amano, Noriaki Ochi, Hirofumi Sato, and Shigeyoshi Sakaki

*J. Am. Chem. Soc.*, **2007**, 129 (26), 8131-8138 • DOI: 10.1021/ja068584d • Publication Date (Web): 12 June 2007

Downloaded from <http://pubs.acs.org> on February 16, 2009



### More About This Article

Additional resources and features associated with this article are available within the HTML version:

- Supporting Information
- Links to the 4 articles that cite this article, as of the time of this article download
- Access to high resolution figures
- Links to articles and content related to this article
- Copyright permission to reproduce figures and/or text from this article

[View the Full Text HTML](#)

### Oxidation Reaction by Xanthine Oxidase. Theoretical Study of Reaction Mechanism

Tatsuo Amano,<sup>†</sup> Noriaki Ochi,<sup>†</sup> Hirofumi Sato,<sup>\*†</sup> and Shigeyoshi Sakaki<sup>\*†,‡</sup>

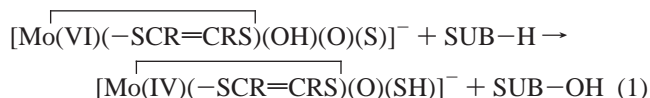
Contribution from the Department of Molecular Engineering, Graduate School of Engineering, Kyoto University, Nishikyo-ku, Kyoto, 615-8510, Japan, and Fukui Institute for Fundamental Chemistry, Kyoto University, Sakyo-ku, Kyoto, 606-7708, Japan

Received November 29, 2006; E-mail: sakaki@moleng.kyoto-u.ac.jp

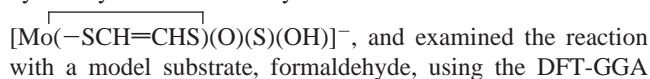
**Abstract:** The oxidation process by molybdenum-containing enzyme, xanthine oxidase, is theoretically studied with a model complex representing the reaction center and a typical benchmark substrate, formamide. Comparisons were systematically made among reaction mechanisms proposed previously. In the concerted and stepwise mechanisms that were theoretically discussed previously, the oxidation reaction takes place with a moderate activation barrier. However, the product is less stable than the reactant complex, which indicates that these mechanisms are unlikely. Moreover, the product of the concerted mechanism is not consistent with the isotope experimental result. In addition to those mechanisms, another mechanism initiated by the deprotonation of the active site was newly investigated here. In the transition state of this reaction, the carbon atom of formamide interacts with the oxo ligand of the Mo center and the hydrogen atom is moving from the carbon atom to the thioxo ligand. This reaction takes place with a moderate activation barrier and considerably large exothermicity. Furthermore, the product by this mechanism is consistent with the isotope experimental result. Also, our computations clearly show that the deprotonation of the active site occurs with considerable exothermicity in the presence of glutamic acid and substrate. The intermediate of the stepwise mechanism could not be optimized in the case of the deprotonated active site. From all these results, it should be concluded that the one-step mechanism with the deprotonated active site is the most plausible.

#### Introduction

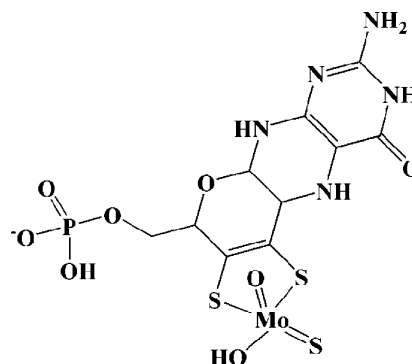
The xanthine oxidase family is a group of molybdenum-containing enzymes, which are widely found in a variety of lives including bacteria and vertebrate animals.<sup>1</sup> On the pathway for the degradation of adenosine monophosphate (AMP) in humans, xanthine oxidase plays a key role, as follows: It oxidizes hypoxanthine to xanthine and then to uric acid. The molybdopterin active center of the enzyme consists of the Mo complex in which the pterin cofactor, thioxo (=S), oxo (=O), and hydroxyl groups coordinate with the Mo center, as shown in Scheme 1. In the oxidation reaction, the Mo center is reduced from hexavalent to quadrivalent, as shown in eq 1. The oxidation



reaction mechanism has been discussed for a long time,<sup>1-7</sup> and several proposals have been presented (Scheme 2). A pioneering theoretical approach to the oxidation mechanism was performed by Voityuk et al.<sup>8</sup> They modeled the active center as



Scheme 1. Active Site of Xanthine Oxidase



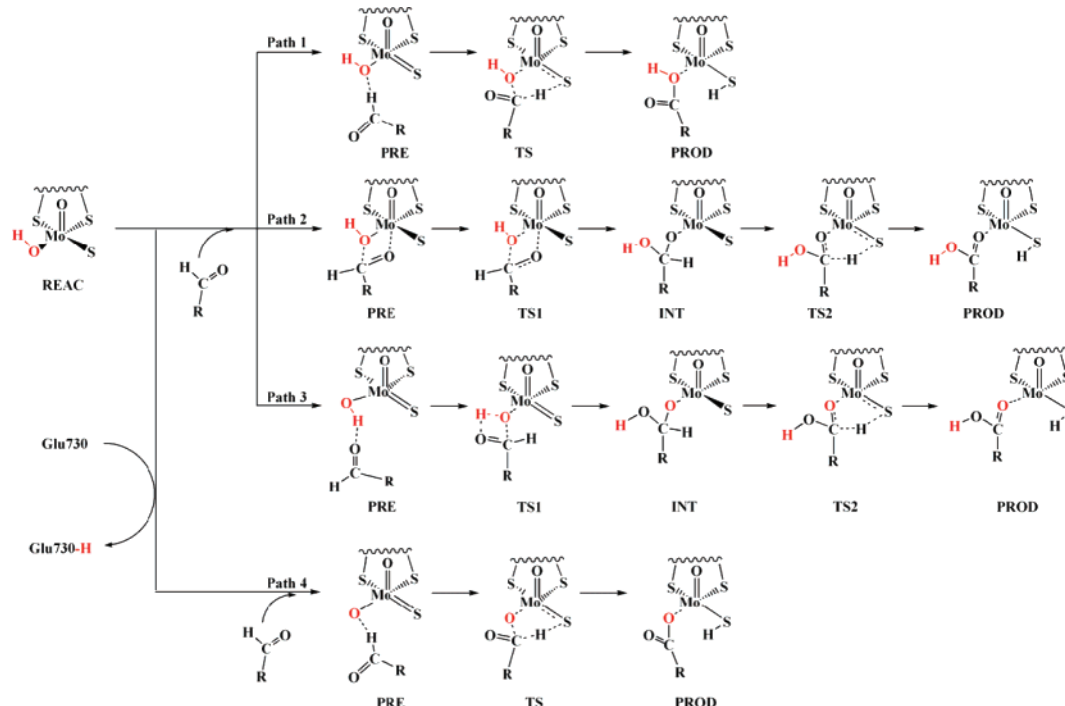
method. The reaction mechanism they proposed is stepwise, in which the hydroxyl group transfers from the active site to the substrate to afford an intermediate and then the hydride transfers from the substrate to the thioxo group (path 3 in Scheme 2). The activation barrier of the hydride shift was evaluated to be 7.7 kcal/mol, while that of the hydroxide transfer was not reported. Hille and his co-workers examined the same model system with a model substrate, formamide, using the MP2

- (2) Huber, R.; Hof, P.; Duarte, R. O.; Moura, J. J. G.; Moura, I.; Liu, M.-Y.; LeGall, J.; Hille, R.; Margarida, A.; Romao, M. *Proc. Natl. Acad. Sci. U.S.A.* **1996**, *93*, 8846.
- (3) Bray, M. R.; Deeth, R. J. *Inorg. Chem.* **1996**, *35*, 5720.
- (4) Enroth, C.; Eger, B. T.; Okamoto, K.; Nishino, T.; Nishino, T.; Pai, E. F. *Proc. Natl. Acad. Sci. U.S.A.* **2000**, *97*, 10723.

<sup>†</sup> Graduate School of Engineering, Kyoto University.

<sup>‡</sup> Fukui Institute for Fundamental Chemistry, Kyoto University.

(1) Hille, R. *Chem. Rev.* **1996**, *96*, 2757.

**Scheme 2.** Possible Mechanisms for Oxidation of Aldehyde

method.<sup>9</sup> Unlike the mechanism investigated in the previous work,<sup>3</sup> they proposed concerted mechanism in which hydroxyl and hydride groups transfer simultaneously (path 1 in Scheme 2). However, the activation barrier (78 kcal/mol) they reported seems to be very high. Very recently, Wu et al. studied the model reactions using the DFT(B3LYP) method,<sup>10</sup> in which four substrates, formaldehyde, acetaldehyde, formamide, and formamidine, were employed as the model of substrate and [Mo(-SCMe=CMeS)(O)(S)(OH)]<sup>-</sup> was adopted as the model of the active site. The activation barriers of the formamide reaction were reported to be 40.0 and 38.6 kcal/mol for the concerted and stepwise mechanisms, respectively (path 1 and path 2 in Scheme 2). It should be noted that these barrier heights are almost half of the value previously reported by Hille et al.<sup>9</sup>

Recently, Hille et al. reported a crucial experimental result on the reaction mechanism of xanthine dehydrogenase.<sup>11</sup> From a mutation experiment, they clearly showed that glutamic acid (Glu730) plays an important role in the oxidation process and suggested that the deprotonation of the hydroxyl group by the glutamic acid (Glu730) necessarily occurs to initiate the reaction (path 4 in Scheme 2). Another crucial result was reported from isotope experiment,<sup>12</sup> in which an <sup>18</sup>O atom was introduced into the hydroxyl group of the Mo active site. Interestingly, the product was bound with the Mo center through the <sup>18</sup>O atom. This indicates that path 2 in Scheme 2 is not likely because the

product of this mechanism coordinates with the Mo center via the carbonyl O atom.

Thus, the reaction mechanism of xanthine oxidase has been still the subject of controversy. Considering these circumstances, here we theoretically investigated the oxidation mechanism of xanthine oxidase with a typical benchmark substrate, formamide. Because the possibility of deprotonation of the hydroxide group was proposed recently,<sup>11</sup> we systematically investigated the concerted and stepwise mechanisms with the protonated and deprotonated active sites. Our purposes here are to clarify which reaction mechanism is the most plausible, what theoretical method should be applied to this reaction, and whether or not the model of active site is reasonable.

### Computational Details and Model

All calculations were performed with the Gaussian 03 program.<sup>13</sup> Population analysis was carried out with the method of Weinhold et al.<sup>14</sup> Geometries were optimized at the DFT(B3LYP) level.<sup>15,16</sup> The core electrons (up to 4d) of Mo were replaced with effective core potentials (ECPs) of LANL2DZ, and its valence electrons were represented with a (541/541/211/1) basis set, where one *f* polarization function was added.<sup>17,18</sup> For C, N, O, and S, the usual 6-31G(d) basis sets were employed.<sup>19a, b</sup> For H atoms that directly participate in the reaction, the 6-31G(d, p) basis set was used,<sup>20</sup> while the usual 6-31G basis set was used for the other H atoms.<sup>21</sup> For P, the (21/21/1) basis

- (5) Ilich, P.; Hille, R. *J. Am. Chem. Soc.* **2002**, *124*, 6796.
- (6) Okamoto, K.; Matsumoto, K.; Hille, R.; Eger, B. T.; Pai, E. F.; Nishino, T. *Proc. Natl. Acad. Sci. U.S.A.* **2004**, *101*, 7931.
- (7) Doonan, C. J.; Stockert, A. L.; Hille, R.; George, G. N. *J. Am. Chem. Soc.* **2005**, *127*, 4518.
- (8) Voityuk, A. A.; Albert, K.; Romao, M. J.; Huber, R.; Rösch, N. *Inorg. Chem.* **1998**, *37*, 176.
- (9) Ilich, P.; Hille, R. *J. Phys. Chem. B* **1999**, *103*, 5406.
- (10) Zhang, X.-H.; Wu, Y. D. *Inorg. Chem.* **2005**, *44*, 1466.
- (11) Leimkuhler, S.; Stockert, A. L.; Igarashi, K.; Nishino, T.; Hille, R. *J. Biol. Chem.* **2004**, *279*, 40437.
- (12) Hemann, C.; Ilich, P.; Stockert, A. L.; Choi, E.-Y.; Hille, R. *J. Phys. Chem. B* **2005**, *109*, 3023.

- (13) Pople, J. A.; et al. *Gaussian 03*, revision C.02; Gaussian, Inc.: Wallingford, CT, 2004.
- (14) Reed, A. E.; Curtis, L. A.; Weinhold, F. *Chem. Rev.* **1988**, *88*, 849 and references therein.
- (15) (a) Becke, A. D. *Phys. Rev. A* **1988**, *38*, 3098. (b) Becke, A. D. *J. Chem. Phys.* **1983**, *98*, 5648.
- (16) Lee, C.; Yang, W.; Parr, R. G. *Phys. Rev. B* **1988**, *37*, 785.
- (17) (a) Hay, P. J.; Wadt, W. R. *J. Chem. Phys.* **1985**, *82*, 299. (b) Couty, M.; Hall, M. B. *J. Comp. Chem.* **1996**, *17*, 1359.
- (18) Ehlers, A. W.; Böhme, M.; Dapprich, S.; Gobbi, A.; Höllwarth, A.; Jonas, V.; Köhler, K. F.; Stegmann, P.; Veldkamp, A.; Frenking, G. *Chem. Phys. Lett.* **1993**, *208*, 111.

**Table 1.** Energy Changes by the Concerted Mechanism<sup>a</sup> with the Protonated Active Site

method	REAC	PRE1	TSa	PRODa	E <sub>a</sub>
(1) BS-1 <sup>b</sup> is used.					
DFT(B3LYP)	0.0 <sup>c</sup>	-13.1	26.2	2.4	39.3
RHF	0.0 <sup>d</sup>	-12.6	25.3	-44.8	37.9
MP2	0.0 <sup>e</sup>	-16.7	54.4	25.9	71.1
MP3	0.0 <sup>f</sup>	-16.2	21.8	-23.3	38.0
MP4(DQ)	0.0 <sup>g</sup>	-31.0	29.0	0.7	60.0
MP4(SDQ)	0.0 <sup>h</sup>	-29.8	35.8	13.9	65.6
MP4(SDTQ)	0.0 <sup>i</sup>	-14.2	73.3	49.6	87.5
CCSD	0.0 <sup>j</sup>	-16.1	25.5	-10.9	41.6
CCSD(T)	0.0 <sup>k</sup>	-16.1	25.0	-0.1	41.1
(2) BS-2 <sup>b</sup> is used.					
DFT(B3LYP)	0.0 <sup>l</sup>	-13.3	28.8	7.1	42.1

<sup>a</sup> Path 1 in Scheme 2. <sup>b</sup> Diffuse functions were not added to N, O, and S atoms in BS-1 but added to them in BS-2. <sup>c</sup> Total energies (in hartree) of the system are <sup>c</sup>-1660.68626, <sup>d</sup>-1655.62349, <sup>e</sup>-1657.67175, <sup>f</sup>-1657.55854, <sup>g</sup>-1657.63459, <sup>h</sup>-1657.70895, <sup>i</sup>-1657.88464, <sup>j</sup>-1657.63102, <sup>k</sup>-1657.73641, and <sup>l</sup>1660.7191.

**Table 2.** Energy Changes by the Stepwise Mechanism<sup>a</sup> with the Protonated Active Site<sup>b</sup>

method	REAC	PRE	TS1	INT	TS2	PROD
B3LYP/BS-1 <sup>c</sup>	0.0	-13.1	25.8	1.9	15.7	-6.4
B3LYP/BS-2 <sup>c</sup>	0.0	-13.3	29.3	4.9	18.4	-1.7
CCSD(T)/BS-1 <sup>c</sup>	0.0	-16.1	25.6	-5.4	9.6	-9.6

<sup>a</sup> Path 3 in Scheme 2. <sup>b</sup> Total energies of the system are given in Table 1. RHF-MP4(SDTQ) energies are in Table S1. <sup>c</sup> Diffuse functions were not added to N, O, and S atoms in BS-1 but added to them in BS-2.

set was employed for the valence electrons,<sup>22,23</sup> where the core electrons of P (up to 2p) were replaced with ECPs.<sup>22</sup> A basis set system consisting of these basis sets is called BS-1. Energy changes were evaluated with DFT(B3LYP), MP2 to MP4, and CCSD(T) methods, using BS-1, to make comparisons of the computational methods. Important intermediates and transition states were recalculated by the DFT method using the 6-31+G(d) basis sets<sup>19a-e</sup> for N, O, and S atoms without any change for the other basis sets. The basis set system with diffuse functions is called BS-2, hereafter. The energy values calculated with the DFT/BS-2 method are presented in the text without any notification.

We employed here two models for the pterin cofactor; one is the simplest model, [-SCH=CHS]<sup>2-</sup>, and the other is a modified pterin cofactor, in which the phosphate moiety was replaced by the PO<sub>2</sub>(OH) group (see Scheme 1). Since the difference in electronic effect between the modified pterin cofactor and the simple model is small, as will be described below, comparisons of reaction mechanisms were made with the simple model.

## Results and Discussion

**Computational Method to Be Applied to Xanthine Oxidase.** First, we applied various computational methods to the concerted reaction mechanism (path 1 of Scheme 2) proposed by Hille et al.<sup>5,9</sup> to clarify what computational method presents reliable results for this reaction. Geometry changes were

**Table 3.** Energy Changes by the Concerted Mechanism<sup>a</sup> with the Deprotonated Active Site in the N-Down Form (above) and in the N-Up Form (below)

method	REAC	PRE	TS	PROD	E <sub>a</sub>
(A) The N-down Form					
B3LYP/BS-1 <sup>b</sup>	0.0 <sup>c</sup>	-24.1	13.6	-27.6	37.7
B3LYP/BS-2 <sup>b</sup>	0.0 <sup>d</sup>	-24.7	12.7	-27.6	27.4
CCSD/BS-1 <sup>b</sup>	-0.0 <sup>e</sup>	-24.7	10.9	-44.9	35.6
CCSD(T)/BS-1 <sup>b</sup>	0.0 <sup>f</sup>	-25.5	9.4	-31.2	34.9
(B) The N-up Form					
B3LYP/BS-1 <sup>b</sup>	0.0 <sup>c</sup>	-26.0	13.8	-27.0	39.8
B3LYP/BS-2 <sup>b</sup>	0.0 <sup>d</sup>	-26.4	13.1	-27.4	39.5
CCSD/BS-1 <sup>b</sup>	0.0 <sup>e</sup>	-26.3	10.9	-45.4	37.2
CCSD(T)/BS-1 <sup>b</sup>	0.0 <sup>f</sup>	-27.2	9.4	-31.8	36.6

<sup>a</sup> Path 4 in Scheme 2. <sup>b</sup> Diffuse functions were not added to N, O, and S atoms in BS-1 but added to them in BS-2. <sup>c</sup> Total energies (in hartree) of the system are <sup>c</sup>-1659.92723, <sup>d</sup>-1660.05671, <sup>e</sup>-1656.90761, <sup>f</sup>-1657.01639.

**Table 4.** Energy Changes by the Concerted Mechanism<sup>a</sup> with the Deprotonated Active Site Including Pterin Cofactor

path	REAC	PRE	TS	PROD	E <sub>a</sub>
(A) DFT(B3LYP)/BS-1 <sup>b</sup>					
N-down	0.0 <sup>c</sup>	-25.1	13.4	-27.8	38.5
N-up	0.0 <sup>d</sup>	-26.9	13.7	-28.9	40.6
(B) DFT(B3LYP)/BS-2 <sup>b</sup>					
N-down	0.0 <sup>e</sup>	-27.3	12.6	-27.5	39.9

<sup>a</sup> Path 4 in Scheme 2. <sup>b</sup> Diffuse functions were not added to N, O, and S atoms in BS-1 but added to them in BS-2. <sup>c</sup> Total energies (in hartree) of the system are <sup>c</sup>-2701.65332, <sup>d</sup>-2701.65332, and <sup>e</sup>-2702.063485.

optimized with the DFT method, of which details will be discussed below. Energy changes were evaluated with various computational methods, where BS-1 was used because the main purpose here is to make comparisons of various computational methods. The activation barrier of this concerted mechanism was evaluated to be about 39 and 41 kcal/mol with the DFT and CCSD(T) methods, respectively, as shown in Table 1, where the activation barrier was defined as an energy difference between the reactant complex and the transition state. However, the MP2 and MP4(SDTQ) calculations provided very large activation barriers of 71 and 88 kcal/mol, respectively (Table 1). These MP2 and MP4(SDTQ)-calculated activation barriers are close to the MP2-calculated value (78 kcal/mol) previously reported by Ilich et al.<sup>5,9</sup>

It is noted that the activation barrier does not converge upon going to MP4 from MP2. This is because the wavefunction of the reactant involves RHF → UHF instability. The instability mainly arises from the (d<sub>π</sub>-p) → (d<sub>π</sub>-p)\* excitation of the Mo=S bond in the reactant. From these results, it should be concluded that the Møller-Plesset perturbation theory cannot be applied to xanthine oxidase. This instability was not observed in DFT wavefunction. The DFT(B3LYP) and CCSD(T) methods provide similar energy profile of this reaction, as shown in Table 1. However, it is noted that the CCSD(T)-calculated reaction energy is significantly different from the CCSD-calculated value while both CCSD and CCSD(T) methods present a similar activation barrier (see the relative energies of the transition state and product in Table 1). In other words, the perturbation method which is used to incorporate the contribution of triple-excitations induces significantly large energy change. This suggests that the perturbation method is not reliable here because a single-reference method fails. Thus, we will present discussion based on DFT-calculated energy changes hereafter (Tables 1–4).

- (19) (a) Hehre, W. J.; Ditchfield, R.; Pople, J. A. *J. Chem. Phys.* **1972**, *56*, 2257. (b) Francl, M. M.; Pietro, W. J.; Hehre, W. J.; Binkley, J. S.; Gordon, M. S.; DeFrees, D. J.; Pople, J. A. *J. Chem. Phys.* **1982**, *77*, 3654. (c) Hariharan, P. C.; Pople, J. A. *Mol. Phys.* **1974**, *27*, 209. (d) Clark, T.; Chandrasekhar, J.; Spitzmuller, G. W.; Schleyer, P. v. R. *J. Comput. Chem.* **1983**, *4*, 294. (e) Frisch, M. J.; Pople, J. A.; Binkley, J. S. *J. Chem. Phys.* **1984**, *80*, 3265.
- (20) Ditchfield, R.; Hehre, W. J.; Pople, J. A. *J. Chem. Phys.* **1971**, *54*, 724.
- (21) Krishnan, R.; Binkley, J. S.; Seeger, R.; Pople, J. A. *J. Chem. Phys.* **1980**, *72*, 650.
- (22) Wadt, W. R.; Hay, P. J. *J. Chem. Phys.* **1985**, *82*, 284.
- (23) Höllwarth, A.; Böhme, M.; Dapprich, S.; Ehlers, A. W.; Gobbi, A.; Jonas, V.; Köhler, K. F.; Stegmann, R.; Veldkamp, A.; Frenking, G. *Chem. Phys. Lett.* **1993**, *208*, 237.

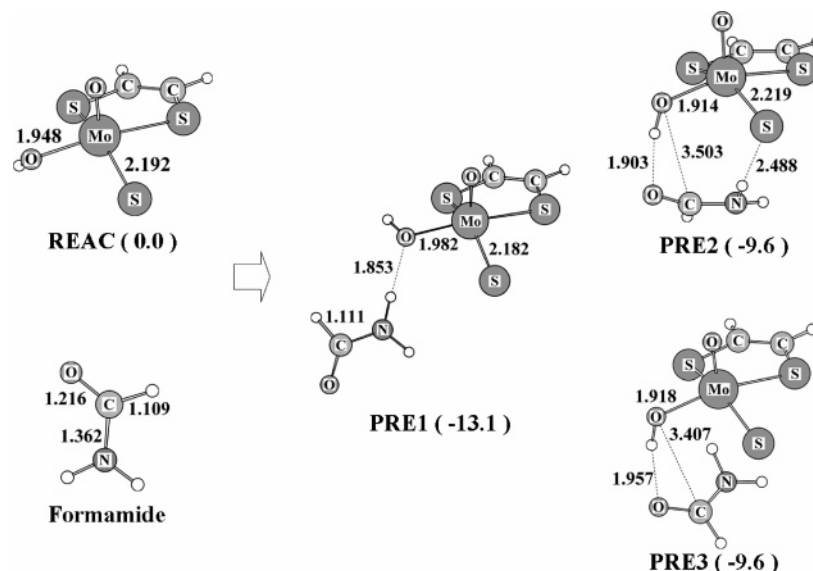
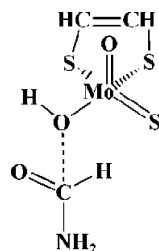


**Figure 1.** Several important H-bonding reactant complexes with bond distances in angstrom. In parentheses are relative energies (in kcal/mol) calculated with the DFT/BS-1 method, where the sum of the reactants is taken to be the standard (energy zero).

**Scheme 3.** Reactant Complex Expected to be Connected to the Transition State



**Hydrogen-Bonding Reactant Complex.** We found three stable structures of the hydrogen-bonding adduct between formamide and the Mo model complex, as shown in Figure 1. In these adducts, formamide does not directly face to the hydroxyl oxygen atom which attacks the carbonyl carbon of formamide in the reaction. In the most stable hydrogen bonding adduct (**PRE1** in Figure 1), the amido hydrogen atom of formamide interacts with the hydroxyl oxygen atom. In the other two, carbonyl oxygen atom of formamide interacts with hydroxyl hydrogen atom (**PRE2** and **PRE3** in Figure 1), while the orientation of formamide is different between them. Both are calculated to be less stable than **PRE1** by 3.5 kcal/mol with the DFT/BS-1 method. We tried to optimize the adduct of Scheme 3, which seems to be connected to the transition state of the reaction, but failed. We, therefore, employed the most stable **PRE1** as the reactant complex of this reaction. **PRE1** was calculated to be more stable than the sum of reactants by 13.1 and 13.3 kcal/mol with the DFT/BS-1 and DFT/BS-2 methods, respectively.

**The Concerted and Stepwise Mechanisms with Protonated Active Site.** We first investigated the concerted reaction mechanism (path 1 in Scheme 2), which has been previously discussed by several groups.<sup>5,9,10</sup> In the concerted mechanism, the hydrogen atom transfers from formamide to the Mo center, concomitantly with which the hydroxyl group transfers from the Mo center to the substrate, as shown in Figure 2. In the transition state **TSa**, the C–H distance considerably lengthens to 1.394 Å by 0.283 Å, while the S–H distance is considerably longer than that of the product **PRODa** by 0.207 Å. Also, the

Mo–OH distance moderately lengthens to 2.109 Å by 0.127 Å. Consistent with the moderately long Mo–OH distance, the C–OH distance is still considerably longer than that of **PRODa** by 0.293 Å. In other words, the H atom is moving halfway toward the S atom but the position of OH is reactant-like. These geometrical features suggest that the H transfer induces the OH transfer in the concerted mechanism. In **PRODa**, the hydroxyl group of the carbamic acid coordinates with the Mo center through its oxygen atom, which is not consistent with the isotope experimental result.<sup>12</sup> The activation barrier is calculated to be 42.1 kcal/mol. It should be noted that the product is much less stable than **PRE1**, as shown in Figure 2. These results indicate that this mechanism is not likely.

In the stepwise mechanism (path 3 in Scheme 2), the first step is the proton transfer from the hydroxide ligand to the carbonyl oxygen of formamide, concomitantly with which the carbonyl carbon atom electrophilically attacks the hydroxyl oxygen atom coordinating with the Mo center, as shown in Figure 3. This process takes place through transition state **TS1b**, to afford an intermediate (**INT1b**). In **TS1b**, the moving proton is considerably distant from the oxygen atom which is bound with the Mo center, but considerably close to the oxygen atom of formamide (see Figure 3). It is also noted that the C–O distance between the carbonyl and hydroxide groups is considerably long. In **INT1b**, the oxygen atom, that was in the hydroxyl group of the reactant, connects the Mo complex and the formamide moiety. We found several isomers of the intermediate with respect to the rotation around the bridging oxygen–carbon axis. The vibrational frequencies of this mode are very small, being ca. 50 cm<sup>-1</sup> (see Supporting Information Figure S1). Their total energies are almost the same, and the barriers among them are very small, being less than 5 kcal/mol. We displayed the most stable structure in Figure 3. In the next process, the hydrogen atom transfers from the formamide carbon atom to the sulfur atom through the transition state (**TS2b**). In **TS2b**, the C–H distance lengthens to 1.403 Å by 0.300 Å but the S–H distance (1.622 Å) is still 0.265 Å longer than that of the product **PRODb**. In other words, the H atom is moving halfway toward the S atom. In **PRODb**, the carbonyl

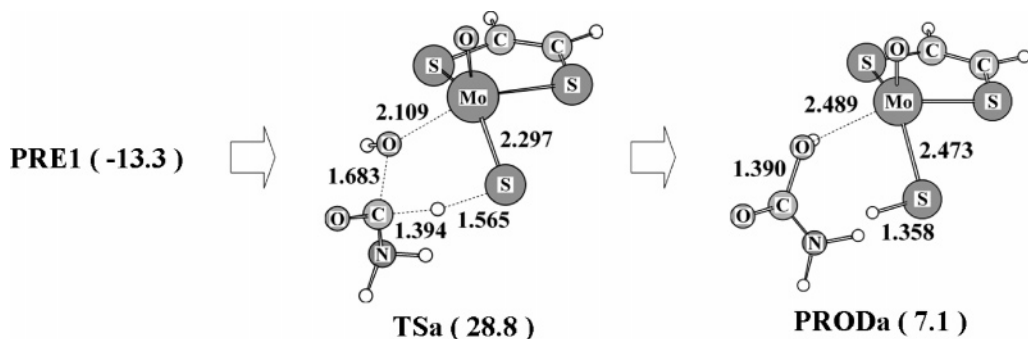


**Figure 2.** Geometry changes by the concerted mechanism with a protonated active site. Bond distances are in angstrom. In parentheses are relative energies (in kcal/mol) calculated with the DFT/BS-2 method, where the sum of the reactants is taken to be the standard (energy zero).

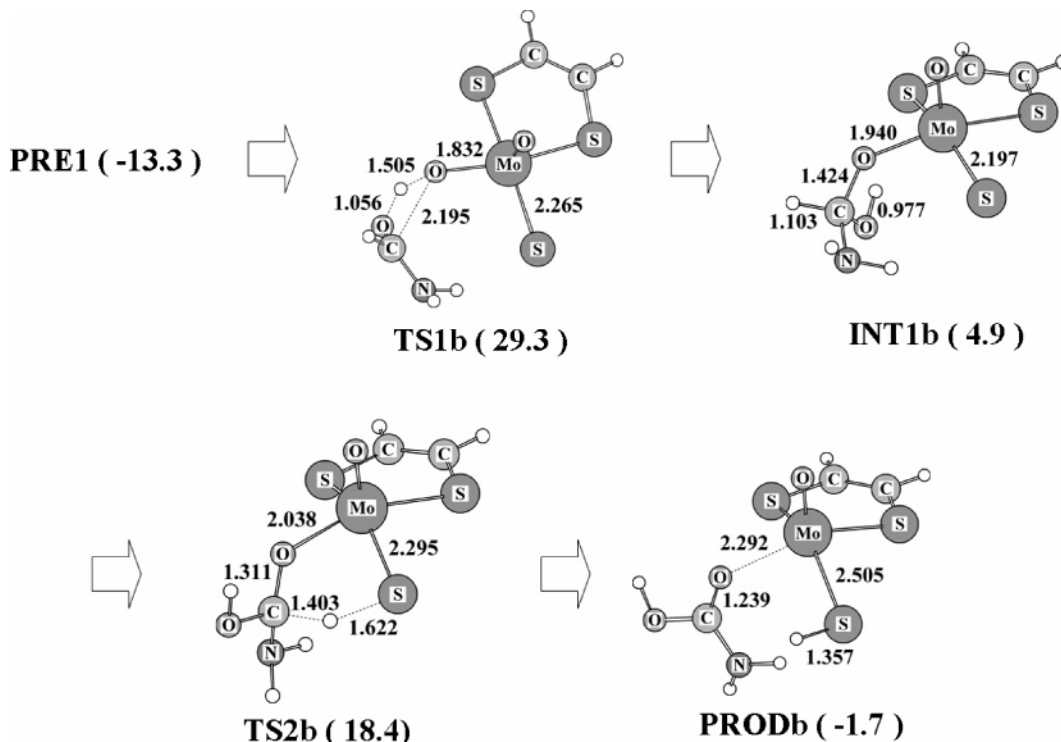


**Figure 3.** Geometry changes by the stepwise mechanism with a protonated active site. Bond distances are in angstrom. In parentheses are relative energies (in kcal/mol) calculated with the DFT/BS-2 method, where the sum of the reactants is taken to be the standard (energy zero).

oxygen atom coordinates with the Mo center, which is consistent with the isotope experimental result<sup>12</sup> because the carbonyl oxygen atom was involved in the basal hydroxyl group of **PRE1**.

The activation energies are calculated to be 42.6 and 13.5 kcal/mol for **TS1b** and **TS2b**, respectively. These results show that the first step is rate-determining. The activation barrier is similar to that of the concerted mechanism. However, it is noted that the product is less stable than **PRE1** in this mechanism, suggesting that this mechanism is unlikely, too.

**Deprotonation of Hydroxide Ligand.** We investigated whether or not the hydroxide ligand of the Mo complex undergoes deprotonation in the presence of the glutamic acid residue. The X-ray structural data<sup>6</sup> represent that two C–O bond lengths of the residue are about 1.25 Å and the Mo–O bond is about 1.97 Å, implying that the ligand is not oxo but hydroxide and that the glutamic acid residue takes an anionic form, glutamate; note the Mo=O distance is about 1.69 Å.<sup>6</sup> These geometrical features indicate that the deprotonation does not occur in Xanthine oxidase.

To reduce the size of the system, we modeled the glutamic acid residue by butanoic acid. The geometries of the molybdopterin moiety and the butanoic acid are taken to be the same as those included in the ONIOM(B3LYP:UFF)-optimized whole protein. In the ONIOM calculation, we used the DFT(B3LYP) method for molybdopterin and butanoic acid moieties, and the MM method for the other part. The sum of deprotonated **PRE** complex and butanoic acid (Mo–O<sup>−</sup>–xanthine + PrCOOH) is 35.1 kcal/mol more stable than the sum of the protonated Mo complex, free xanthine, and butanoate (Mo–OH + xanthine + PrCOO<sup>−</sup>) (eq 2). However, the sum of the deprotonated Mo complex and butanoic acid (Mo–O<sup>−</sup> + PrCOOH) is only 2.5 kcal/mol more stable than the sum of the protonated Mo

(24) The experiment indicated that Glu730 is about 4 Å distant from the Mo active site.<sup>6</sup> The deprotonation of the Mo active center changes the anion form of Glu730 to the protonated neutral form. This means that the proton does not exist around the Mo active center. It is likely that the neutral carboxylic acid little influences the reaction of the active site when it is about 4 Å distant from the active site.

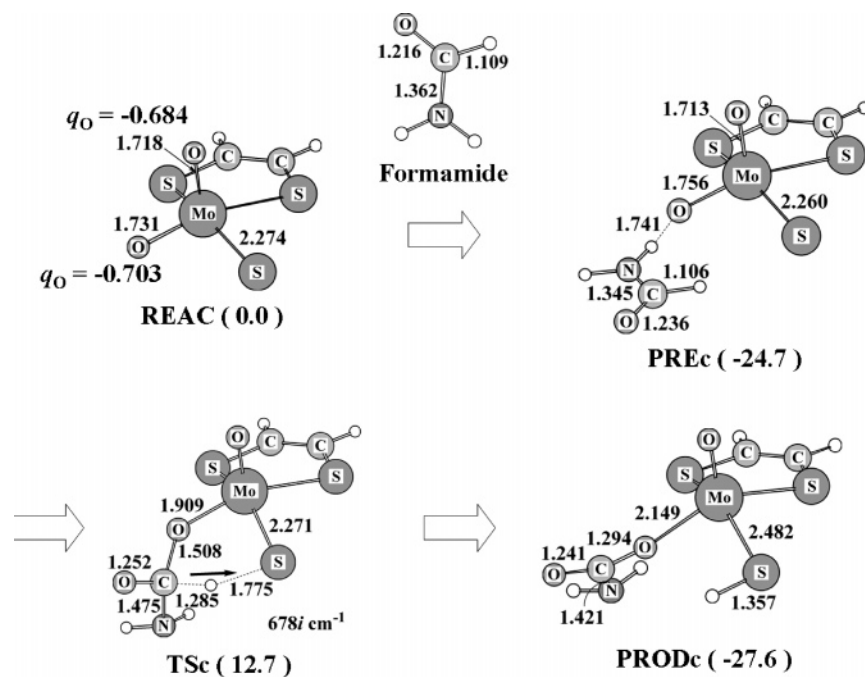


**Figure 4.** Geometry changes with a deprotonated active site in the N-down conformation. Bond distances are in angstrom. In parentheses are relative energies (in kcal/mol) calculated with the DFT/BS-2 method, where the sum of the reactants is taken to be the standard (energy zero). The  $q_O$  represents the NAO charge on the oxo ligand.

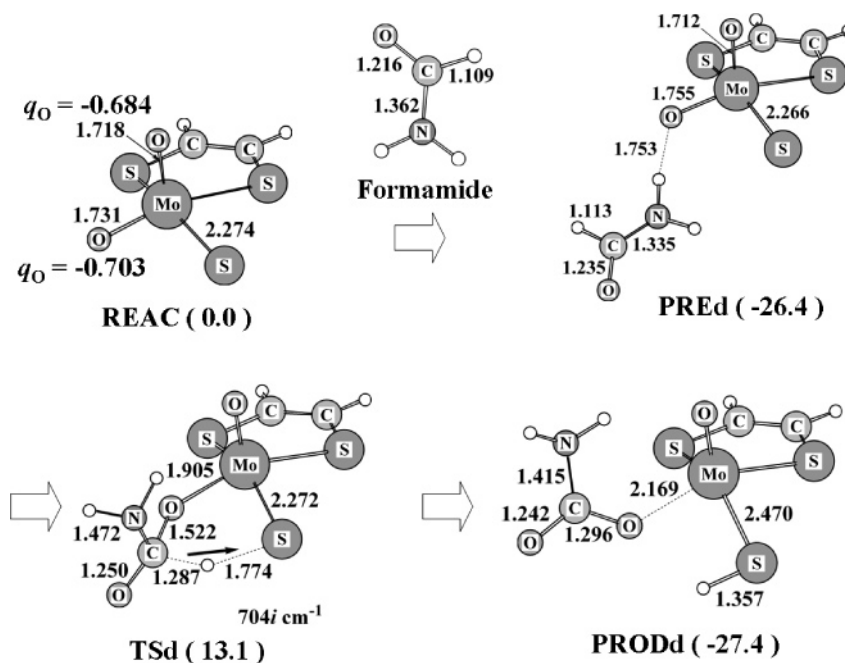
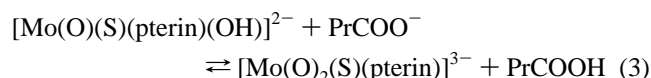
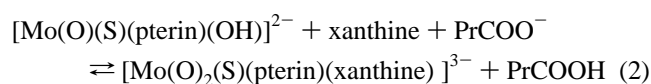


**Figure 5.** Geometry changes with a deprotonated active site in the N-up conformation. Bond distances are in angstrom. In parentheses are relative energies (in kcal/mol) calculated with the DFT/BS-2 method, where the sum of the reactants is taken to be the standard (energy zero). The  $q_O$  represents NAO charge on the oxo ligand.

complex and butanoate ( $\text{Mo-OH} + \text{PrCOO}^-$ ) in the absence of xanthine (eq 3).<sup>24</sup>



These results suggest that the deprotonation of the hydroxide ligand easily occurs with the approach of the substrate. This

suggestion is consistent with the X-ray structural data which show that the deprotonation does not occur in xanthine oxidase in the absence of substrate,<sup>6</sup> as described above.

**Reaction Mechanism with Deprotonated Active Site (Path 4 in Scheme 2).** Because the deprotonation of the active site easily occurs in the presence of substrate, as discussed above, we investigated the reaction mechanism with the deprotonated active site.<sup>25</sup> Two stable reactant complexes, **PREc** and **PREd** (Figures 4 and 5), were optimized in the deprotonated Mo complex. Both of them are understood in terms of the hydrogen-

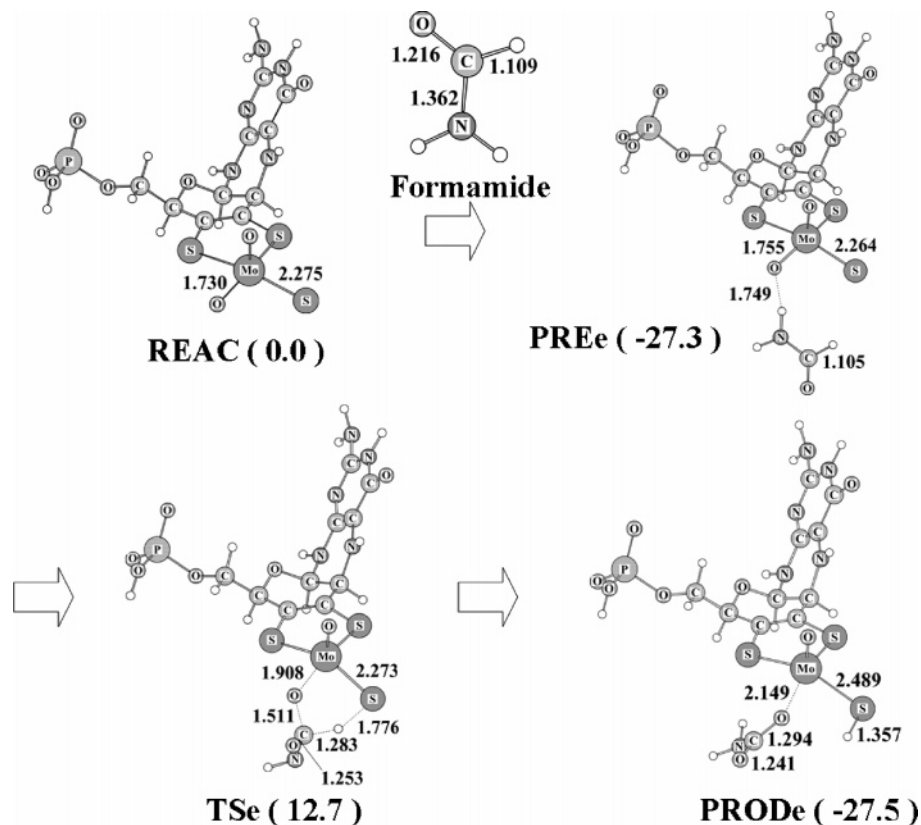


**Figure 6.** Geometry changes by the reaction with a deprotonated active site in the N-down conformation including the pterin cofactor. Bond distances are in angstrom. In parentheses are relative energies (in kcal/mol) calculated with the DFT/BS-2 method, where sum of the reactants is taken to be the standard (energy zero).

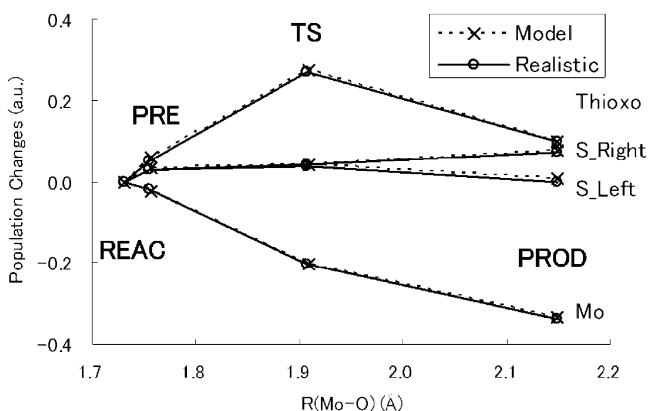


**Figure 7.** Population changes of selected atoms by the oxidation of formamide. Positive change represents a gain of NBO charge relative to the reactants and vice versa.

bonding complex in which the amide hydrogen atom coordinates with the deprotonated oxygen atom. The difference between them is only the orientation of formamide: **PREc** takes the N-down form and **PREd** takes the N-up form. The stabilization energy by formamide coordination is a little different between

them. Starting from **PREc** and **PREd**, the reaction proceeds through transition states **TSc** and **TSd**, respectively (Figures 4 and 5). We confirmed that these transition states are directly connected with the corresponding reactant complex and the product by pseudo-IRC calculation.<sup>26</sup> Neither intermediate nor barrier was observed between the transition state and the product and between the transition state and the reactant complex.

**TSc** is essentially the same as **TSd**; the only one difference is the direction of the C–N bond. Thus, we will present discussion about geometrical features of **TSc**. In **TSc**, the Mo–O distance considerably lengthens to 1.909 Å by 0.153 Å and the C–O distance is longer than that of the product, **PRODc**, by 0.214 Å. Also the C–H distance considerably lengthens to 1.285 Å by 0.179 Å, while the S–H distance is much longer than that of **PRODc** by 0.418 Å. These geometrical features suggest that the position of the oxygen atom is product-like but the position of the hydrogen atom is reactant-like; in other words, the oxygen transfer induces the hydrogen transfer. In **PRODc**, it should be noted that carbamate anion coordinates with the Mo center through the oxygen atom that was originally in the basal oxo ligand of the reactant complex. This geometry is consistent with the isotope experiment which showed that the basal OH group is labeled by the <sup>18</sup>O atom and the product coordinates with the Mo center through the <sup>18</sup>O atom.<sup>12</sup>

Energy changes by the reaction via **TSc** and **TSd** are similar; for instance, the activation barrier is evaluated to be 37.4 and 39.5 kcal/mol for **TSc** and **TSd**, respectively. These activation barriers are moderately smaller than that (42.1 kcal/mol) of the

(25) (a) The exothermicities of eqs 3 and 4 are evaluated to be 11.3 and 4.2 kcal/mol, respectively, with the PCM method, where the  $\epsilon$  value of 4.0 was employed because this value is often used to mimic the atmosphere of protein in PCM calculations. These results indicate that eq 2 is still much more exothermic than eq 3, though the difference in exothermicity between eqs 2 and 3 considerably decreases in the PCM calculation. Thus, our conclusion does not change in the PCM calculation. (b) The significant decrease in the exothermicity of eq 2 by the PCM calculation is understood by considering that the solvation induces a significantly larger stabilization energy of the product of eq 3 than that of eq 2 because the anionic O atom is exposed to solvent in the product of eq 3 but covered with the substrate in the product of eq 2.

(26) Careful geometry optimization starting from **TSc** leads to **PREc** and **PRODc**.



concerted mechanism (path 1 in Scheme 2) with the protonated active site. However, the reaction by the deprotonated species is considerably exothermic relative to the sum of reactants and moderately relative to the reactant complex, as shown in Figures 4 and 5, in contrast to the reaction by the protonated species which is considerably endothermic relative to the reactant complex (Figures 2 and 3). It should be concluded that the one-step reaction by the deprotonated active site (path 4 in Scheme 2) is the most plausible mechanism of the reaction by xanthine oxidase.

We could not find the stepwise reaction course in the case of the deprotonated active site; we tried to optimize an intermediate corresponding to **INTb**, but failed. It is concluded that only the one-step mechanism is possible in the reaction of formamide with the deprotonated active site.

At the end of this section, we wish to mention that the possibility that the axial Mo–O moiety reacts with formamide is very small. One of the important reasons is that the X-ray structure analysis showed the lack of enough space for the substrate to approach the Mo center from the axial direction.<sup>6</sup> The isotope experiment also reported that the <sup>18</sup>O atom was incorporated only into the basal position and that the product contained the <sup>18</sup>O atom,<sup>12</sup> indicating that the basal oxygen atom reacted with the substrate. In addition, our computational results suggest that the basal oxygen atom is more reactive than the axial oxygen atom in the nucleophilic attack as follows: the p orbital of the basal oxygen atom largely contributes to the next HOMO and HOMO-2,<sup>27</sup> while the p orbital of the axial oxygen atom contributes little to these high-energy MOs (see Supporting Information Figure S2 for these orbital pictures). The basal O atomic population (−0.7.03e) is more negative than the axial O atomic population (−0.684e), while the difference is not large. From these results, it is reasonably concluded that not the axial oxygen atom but the basal oxygen atom reacts with substrate.

**Model of Pterin Cofactor.** Another important issue to be investigated is the effect of pterin cofactor, because it is modeled here by the simple ethylene dithiolate anion. We investigated the one-step mechanism (path 4 in Scheme 2) with the deprotonated active site including the pterin cofactor, because this mechanism is considered to be the most plausible, as discussed above.

All of their structures around the active site resemble well those of the simple model system, as shown in Figure 6. Table 4 lists the energy changes of the system including the pterin cofactor, where only the results with the DFT method are shown because the system is too large to perform CCSD(T) calculation. The barrier height and the energy of the reaction are very close to those of the simple model system. The population changes

of selected atoms are a little different between the model and realistic systems, as you can see in Figure 7. From all these results, it is concluded that the simple model presents reliable results.

## Conclusions

Several plausible reaction mechanisms of the oxidation process by xanthine oxidase, which were previously proposed and theoretically investigated, were reinvestigated here with a typical model substrate, formamide. In both concerted and stepwise mechanisms (paths 1 and 3 in Scheme 2) that have been discussed by Hille et al.<sup>5,9</sup> and Wu et al.,<sup>10</sup> the activation barrier is about 40 kcal/mol and the product is less stable than the reactant complex, when the active site does not undergo deprotonation. Moreover, the geometry of the product of the concerted mechanism is not consistent with the isotope experimental result.<sup>12</sup> In addition, we theoretically investigated the reaction mechanism with the deprotonated Mo complex which was experimentally proposed but has not been theoretically investigated yet. The deprotonation of the active site easily occurs in the presence of glutamic acid and substrate, compared to the deprotonation in the absence of substrate. The oxidation reaction through the one-step mechanism (path 4 in Scheme 2) occurs with a similar activation barrier to those of the protonated active site. It should be noted here that although the product is less stable than the reactant complex in both concerted and stepwise mechanisms by the protonated active site, the product is more stable than the reactant complex in the one-step mechanism by the deprotonated active site. The reason of the exothermicity is easily understood in terms of the strong interaction between Mo and carbamate. It should also be noted that the product in the one-step mechanism with the deprotonated active site is consistent with the isotope experimental results.<sup>12</sup> The intermediate in the stepwise mechanism could not be optimized in the case of the reaction of formamide with deprotonated active site. From these results, it is clearly concluded that the oxidation reaction proceeds by the deprotonated active site through the one-step mechanism.

**Acknowledgment.** We would like to thank Professor Teizo Kitagawa (IMS, Japan) for important discussions on our results. We acknowledge financial support by the Grant-in Aid for Scientific Research on Priority Areas “Molecular Theory for Real Systems” (No. 461) and “Water and biomolecule” (No. 430) and by the Grant-in Aid for Basic area (No. 18350005) and Encouragement of Young Scientists (No. 17750012) from the Ministry of Education, Science, Culture, and Sports.

**Supporting Information Available:** Complete ref 13; Cartesian coordinates of important species including transition states; geometries of intermediates in stepwise mechanism with protonated active site. This material is available free of charge via the Internet at <http://pubs.acs.org>.

JA068584D

(27) The HOMO is the  $\pi$  orbital of the C=C double bond of  $[-SCH=CHS-]^{2-}$ .